Chemosphere 145 (2016) 351–359

Contents lists available at ScienceDirect

Chemosphere

journal homepage: www.elsevier.com/locate/chemosphere

Treatment of crystallized-fruit wastewater by UV-A LED photo-Fenton and coagulation–flocculation

Jorge Rodríguez-Chueca [a], Carlos Amor [a], José R. Fernandes [b, c], Pedro B. Tavares [a], Marco S. Lucas [a, d, *], José A. Peres [a]

[a] Centro de Química de Vila Real, Departamento de Química, UTAD – Universidade de Trás-os-Montes e Alto Douro, 5000-801 Vila Real, Portugal
[b] Departamento de Física, UTAD – Universidade de Trás-os-Montes e Alto Douro, 5000-801 Vila Real, Portugal
[c] INESC-TEC, Rua do Campo Alegre, 687, 4169-007 Porto, Portugal
[d] Environmental Nanocatalysis and Photoreaction Engineering, Department of Chemical Engineering, Loughborough University, Loughborough LE11 3TU, United Kingdom

HIGHLIGHTS

- First report on CFW treatment with UV-A LED photo-Fenton.
- RSM was applied to achieve the optimal conditions for UV-A LED photo-Fenton.
- Combining UV-A LED photo-Fenton and CFD allow achieve a COD removal greater than 80%.
- UV-A LED photo-Fenton and CFD increases the CFW biodegradability ($BOD_5/COD > 0.4$).

ARTICLE INFO

Article history:
Received 18 July 2015
Received in revised form
19 October 2015
Accepted 23 November 2015
Available online 12 December 2015

Handling Editor: Jun Huang

Keywords:
Biodegradability
Coagulation/flocculation
Crystallized-fruit wastewater
Photo-Fenton
UV-A LED

ABSTRACT

This work reports the treatment of crystallized-fruit effluents, characterized by a very low biodegradability (BOD_5/COD <0.19), through the application of a UV-A LED photo-Fenton process. Firstly, a Box-Behnken design of Response Surface Methodology was applied to achieve the optimal conditions for the UV-A LED photo-Fenton process, trying to maximize the efficiency by saving chemicals and time. Under the optimal conditions ($[H_2O_2] = 5459$ mg/L; $[Fe^{3+}] = 286$ mg/L; time >180 min), a COD removal of 45, 64 and 74% was achieved after 360 min, using an irradiance of 23, 70 and 85 W/m^2 respectively. Then a combination of UV-A LED photo-Fenton with coagulation–flocculation–decantation attained a higher COD removal (80%), as well as almost total removal of turbidity (99%) and total suspended solids (95%). Subsequent biodegradability of treated effluents increased, allowing the application of a biological treatment step after the photochemical/CFD with 85 W/m^2.

1. Introduction

The crystallized-fruit industry annually generates large volumes of wastewater, mainly from several washing and cooking operations of fresh fruits in syrup (water and sugar) as well as the rinsing of tanks, barrels and other equipment. This industrial effluent is characterized by a high seasonal variability, high organic load and unpleasant odour. Conventional treatments available, such as biological processes, in Municipal Wastewater Treatment Plants (MWWTP) are susceptible to several constraints due to the low biodegradability and high organic load of this wastewater.

In order to overcome the limitations of biological processes, physical–chemical treatments have been envisaged as promising alternatives to efficiently remove organic matter, suspended solids and turbidity (Amor et al., 2015). In this context, Advanced Oxidation Processes (AOPs), like H_2O_2/UV-C, heterogeneous photocatalysis, photo-Fenton and H_2O_2/O_3, have been proposed as valuable approaches for water and wastewater treatment (Sichel et al., 2007; Polo-López et al., 2011; Lanao et al., 2012; Rodríguez-

* Corresponding author. Environmental Nanocatalysis and Photoreaction Engineering, Department of Chemical Engineering, Loughborough University, Loughborough LE11 3TU, United Kingdom.
E-mail addresses: m.p.lucas@lboro.ac.uk, mlucas@utad.pt (M.S. Lucas).

http://dx.doi.org/10.1016/j.chemosphere.2015.11.092
0045-6535/

Chueca et al., 2012) due to their efficiency in the generation of hydroxyl radicals (HO•). These highly oxidant species can oxidize almost all organic compounds and inactivate a wide range of microorganisms. AOPs are reported to have been successfully used for the removal of dyes and pigments (Wang et al., 2015); in the treatment of landfill leachates (Cassano et al., 2011; Amor et al., 2015); fresh surface water and drinking water (Mosteo et al., 2009; Lanao et al., 2010); urban wastewater effluents (Rodríguez-Chueca et al., 2014); and also in the paper (Lucas et al., 2012); cork (De Torres-Socías et al., 2013); and agri-food industries (Durán et al., 2012; Chatzisymeon et al., 2013; Velegraki and Mantzavinos, 2015).

Fenton's reagent oxidation is a homogeneous catalytic oxidation process that uses a mixture of hydrogen peroxide and ferrous ions. In an acid environment, the addition of hydrogen peroxide to an aqueous system containing an organic substrate and ferrous ions produces a complex redox reaction (Kuo, 1992; Walling, 1998; Peres et al., 2004). The ferrous ions initiate and catalyze the decomposition of H_2O_2, resulting in the generation of hydroxyl radicals, HO• (Chen and Pignatello, 1997).

The production of HO• is greatly increased by UV–vis radiation up to a wavelength of 600 nm. Photo-Fenton produces hydroxyl radicals via a series of catalytic cycle reactions with iron (Fe^{2+} and Fe^{3+}), H_2O_2, and UV radiation. The highest photo-Fenton efficiency is found at pH 2.8 (Pignatello et al., 2006), since iron salts precipitate far from this pH value. These reactions can be summarized as follows:

$$Fe^{2+} + H_2O_2 \rightarrow Fe^{3+} + OH^- + HO^{\bullet} \ (k = 70\ M^{-1}\ s^{-1}) \quad (1)$$

$$Fe(OH)^{2+} + h\nu \rightarrow Fe^{2+} + HO^{\bullet} \quad (2)$$

Different UV radiation sources to assist photo-Fenton treatments, especially low and medium pressure mercury lamps, have been reported in recent years, but their high operational cost associated with large energy consumption and their toxicity are important drawbacks. In view of this, UV-Light-emitting diodes (LEDs) lamps, which are more efficient and more ecofriendly, present a serious alternative to mercury lamps and solar radiation. Semiconductor LEDs technology are a directional light source with maximum intensity at an angle almost perpendicular to the surface emission. Although at a relatively high cost, LEDs lamps have several advantages when compared to traditional UV lamps – they do not over heat and have a longer lifetime, lower energy consumption and higher efficiency (Rojviroon et al., 2012; Natarajan et al., 2011).

When LEDs lamps are activated, the electrons and holes are directed to *p-n* junctions, suffering a recombination and emitting light (electroluminescence). This recombination compromises the coupling of electrons and holes become more stable to release excess energy by photon emission. In fact, almost all the electrical energy is converted into light energy (Natarajan et al., 2011). As all emitted photons have approximately the same frequency, this implies that the light is monochromatic, thus the wavelength depends on the semiconductor material used. UV LEDs have been increasingly used as they can be applied in several different processes, such as the degradation of chemicals and inactivation of microorganisms (Natarajan et al., 2011).

The main purpose of this research was to optimize the experimental conditions (reaction time, Fe^{3+}, and H_2O_2 dosages) of UV-A LED photo-Fenton treatments by means of a Response Surface Methodology (RSM) model. This optimisation was followed by an evaluation of the combination of a UV-A LED photo-Fenton treatment with a CFD in crystallized-fruit industry wastewater degradation.

2. Materials and methods

2.1. Samples

Crystallized-fruit wastewater (CFW) samples were collected at a company located in the North of Portugal. This company is the market leader of crystallized-fruit production for baking, jam and quince jelly in Portugal. The production process requires a high amount of water to wash and cook of the fruits.

The main fruits used in the industrial process are pumpkins, carrots, pears, oranges, quinces, apples, cherries and figs. These fruits are conserved in baths of sodium bisulphite solutions before their handling. This processing stage promotes the generation of a high reducer wastewater. The physicochemical characteristics of the crystallized-fruit wastewater are summarized in Table 1. The large differences observed in the physicochemical parameters, mainly in terms of pH, oxidation potential, COD and BOD_5, of the three different samples are a consequence of: i) the different productive process in each sample time; ii) the elementary operation of the WWTP of the factory, which relied solely on pH correction with NaOH and aeration of samples in order to remove the sodium bisulfite used to preserve the fruits.

2.2. Analytical determinations

Different physicochemical parameters such as pH, conductivity, redox potential, turbidity, Total Suspended Solids (TSS), Volatile Suspended Solids (VSS), Chemical Oxygen Demand (COD), Total Polyphenols (TP) and Cationic and Anionic concentration were analyzed to characterise the sample. In addition, values of COD, TSS and Turbidity were analyzed during the treatments in order to assess the efficiency of the treatments.

Chemical Oxygen Demand was measured according to the 410.4 Method of the Environmental Protection Agency of USA, using a HACH DR/2400 portable spectrophotometer. BOD_5 was checked and measured according to the 5-Day BOD Test (Standard Method 5210B) using OxiTop® Control respirometer. The pH and redox potential were determined by a HANNA pH 209 laboratory meter following the Standard Method 4500-H+-B and 2580 respectively, while conductivity was measured by a Crison Basic as indicated in ISO 7888:1985. Turbidity was measured according to ISO 7027:1999 using a HACH 2100 IS Turbidimeter. Total Suspended Solids (TSS) were measured by spectrophotometry according to Standard Method 2540D using a HACH DR/2400 portable spectrophotometer, while Volatile Suspended Solids (VSS) were measured using Standard Method 2540-E. In addition, Total Polyphenols concentration (TP), (mg gallic acid/L), was determined by spectrophotometry using the Folin-Ciocalteu reagent (Merck) (Singleton and Rossi, 1965). UV–vis measurements were performed using a Jasco V-530 UV/VIS spectrophotometer. Finally, the anionic analysis was carried out according to D4327 and D6919-09 ASTM International Standards for anions and cations respectively, using a Dionex AS modelo ICS-3000 Detector Chromatography for anions determination, while for cationic determination, a Thermo Scientific Ice 3000 Series AA Spectrometer and an ATI Unicam Solaar 939 Atomic Absorption Spectrometer for the concentrations of mg/L and μg/L were used respectively.

2.3. Reagents

Fenton and photo-Fenton treatments were carried out with different dosages of $FeCl_3 \cdot 6H_2O$ (Merck) and H_2O_2 (30% w/w, Panreac) used as reagent grade. In addition, H_2SO_4 (Scharlau) and NaOH (BDH Prolabo®) aqueous solutions were applied for pH adjustment. Na_2SO_3 (Merck) was used to quench the hydroxyl

Table 1
Physicochemical characteristics of crystallized-fruit wastewater.

Parameter	Values		
	Sample A (02/2014)	Sample B (05/2014)	Sample C (07/2014)
pH (Sorensen scale)	9.78	3.50	6.95
E^o (mV)	−140	212	17
Conductivity (μS/cm)	3820	8304	8578
Turbidity (NTU)	410	359	633
Total suspended solids (mg/L)	1100	1420	1850
Volatile suspended solids (mg/L)	125	265	–
COD (mg O_2/L)	22 932	20 902	35 369
BOD_5 (mg O_2/L)	1400	3300	6600
Biodegradability (BOD_5/COD)	0.06	0.16	0.19
Polyphenols (mg gallic acid/L)	142	403	384
Absorbance at 254 nm (diluted 1:25)	0.265	0.323	0.409
Absorbance at 254 nm (diluted 1:10)	0.539	0.708	0.927
Hardness (mg $CaCO_3$/L)	135	219	228
Chloride (mg Cl^-/L)	824	1073	1281
Nitrite (mg NO_2^-/L)	453	0.07	0.01
Nitrate (mg NO_3^-/L)	168	49.3	88.8
Phosphates (mg PO_4^{3-}/L)	143	n.d.	n.d.
Sulphates (mg SO_4^{2-}/L)	80.5	272.5	n.d.
Calcium (mg Ca^{2+}/L)	36.1	48.6	39.2
Iron (mg Fe^{2+}/L)	87	3.0	2.2
Magnesium (mg Mg^{2+}/L)	10.8	23.8	31.6
Potassium (mg K^+/L)	2850	222	224
Sodium (mg Na^+/L)	901	2766	2632
Aluminium (mg Al^{3+}/L)	7.2	28.9	37.1
Arsenic (μg As/L)	7	46	62
Copper (μg Cu^{2+}/L)	81	21	25
Manganese (mg Mn^{2+}/L)	46	0.16	0.08

radicals action before analyses. The titanium (IV) oxysulfate solution (Riedel-de Haën, Germany) was used as received in order to analyse the concentration of H_2O_2. Finally, different inorganic ($FeSO_4 \cdot 7H_2O$, $FeCl_3 \cdot 6H_2O$, $Al_2(SO_4)_3$, $Ca(OH)_2$ and aluminium chlorohydrate (Kemira Ibérica) and organics (QT100 and QTH100 (Grove Chemicals)) coagulants were used in coagulation–flocculation processes.

2.4. Radiation source

All experiments were carried out in a batch mode lab-scale prototype reactor and illuminated with two different UV-A LED systems. The first UV LED photo-system applied was a matrix of 96 Indium Gallium Nitride (InGaN) LEDs lamps (Roithner RLS-UV370E), with an illuminated area of 11 × 7 cm^2. These LED lamps had a light peak emission wavelength at 370 nm, and the nominal consumption of each LED lamp was 80 mW operating at 20 mA. The total optical power emitted was approximately 100 mW, depending on the root mean square (RMS) current intensity supplied. The system irradiance was measured using a UV enhanced Si-photodetector (ThorLabs PDA155) in a configuration that replicated the one used in the photoreactor. In this system the output optical power was controlled using a pulse width modulation (PWM) circuit. The RMS current intensity was measured with a multimeter (UniVolt DT-64).

The second UV LED system was developed with 12 InGaN LED lamps (Roithner APG2C1-365E LEDS) with a light peak emission wavelength at 365 nm. The nominal consumption of each LED lamp was 1.4 W, for an applied current of 350 mA. The output optical power was controlled by maintaining the forward current constant using a power MOSFET in six different current settings.

The treatments were carried out in two UV-A LED photo-systems. The first one used a RMS current intensity of 240 mA, corresponding to a UV irradiance of 23 W/m^2 and a photon flux of 5.53 × 10^{-7} E/s. In the second photo-system current intensities of 262 and 327 mA were applied, corresponding to an UV irradiance of 70 and 85 W/m^2, respectively, and a photon flux of 1.68 × 10^{-6} and 2.04 × 10^{-6} E/s, respectively.

Fig. S1 (Supplementary material) shows the two UV-A LED photosystems and a diagram of the set-up experiments.

2.5. Experimental procedure

The different experiments were carried out in a batch UV-A LED photoreactor. The pH was adjusted to 3, using H_2SO_4 and a 209 pH Meter from Hanna Instruments. Then, the $FeCl_3 \cdot 6H_2O$ dosage (60–300 mg/L) was added to the effluent. Hydrogen peroxide (200–5500 mg/L) was directly added to the photoreactor at the beginning of each experiment. During each experiment the samples were withdrawn at different intervals and analysed. The H_2O_2 concentration was measured in a spectrophotometer (Jasco V-530) at 410 nm according to DIN 38409 H15, based on the formation of a yellow complex from the reaction of titanium (IV) oxysulphate with H_2O_2. The titanium (IV) oxysulphate method displays a detection limit of 0.1 mg/L. The signal was read after 5 min incubation time against a H_2O_2 standard curve from 0.1 to 100 mg/L H_2O_2. The Na_2SO_3 was added to water samples for the elimination of residual hydrogen peroxide. Temperature and pH were also monitored. Total polyphenols were monitored using the Folin-Ciocalteau method (Singleton and Rossi, 1965). The chemical oxygen demand (COD), biochemical oxygen demand (BOD_5) and total and volatile solids were monitored according to the Standard Methods (Eaton et al., 2005). Moreover, the total iron concentration was measured using the phenanthroline method. Each sample was mixed with 1 mL of 1,10-phenanthroline (1 g/L) and 1 mL of buffer solution according to ISO 6332 regarding the assessment of dissolved Fe^{2+} and total iron (Fe_{total}) concentrations. The coloured complex formed was measured with a spectrophotometer (Jasco V-530) at 510 nm. The concentrations of Fe^{2+} and Fe_{total} were determined using dedicated calibration curves. The temperature

remained constant around 21 °C. All assays were carried out in duplicates and results are presented as mean ± standard deviation. Previous studies of coagulation–flocculation–decantation optimization carried out in our research work (data not shown) demonstrated that the best coagulant was $FeCl_3 \cdot 6H_2O$ at neutral pH (pH 7). In addition, the best yields, mainly in terms of suspended solids and turbidity removal, were observed when CFD was performed after photo-Fenton treatments, because in this way, sludge generated (mainly composed of ferric hydroxides) is removed after the Fenton treatments. Therefore, the CFD processes were carried out at pH 7, after the photo-Fenton treatment and using the remaining iron.

A Jar-Test (ISCO) was used to first produce a rapid agitation (200 rpm) for 3 min, where destabilization of the colloids occurred. This was followed by a slow agitation (40 rpm) period of 15 min. Finally, to promote the formation and precipitation of flocs, a decantation period of 60 min was allowed.

2.6. Experimental design

A Box-Behnken design was employed to evaluate the effect of different parameters on the UV-A LED photo-Fenton treatment of crystallized-fruit effluents, such as H_2O_2 (mg/L, X_1) and Fe^{3+} (mg/L, X_2) concentration, and reaction time (min, X_3). For this study, 15 UV-LED photo-Fenton experiments were performed. The levels considered for the Box-Behnken design are listed in Table 2a. The treatment schedule (Table 2b) was arranged to allow an appropriate regression model. All experiments were carried out in triplicate. Three replicates at the center of the design were used (Experiments 1, 4, and 15). Experiments were randomized to maximize the efforts of unexplained variability in the observed response due to external factors.

Table 2
(a) Symbols and coded factor levels for the considered variables. (b) Box-Behnken design: effect of operational variables on COD removal yield ($[H_2O_2]$ = 1100–5500 mg/L; $[Fe^{3+}]$ = 60–300 mg/L; reaction time = 30–180 min).

(a)

Independent variables	Coded	Levels		
		−1	0	1
$[H_2O_2]$ (mg/L)	X_1	1100	3300	5500
$[Fe^{3+}]$ (mg/L)	X_2	60	180	300
Reaction time (min)	X_3	30	105	180

(b)

Assay	Coded level			Response values	
	$[H_2O_2]$ (mg/L)	$[Fe^{3+}]$ (mg/L)	Time (min)	COD removal (%)	
	X_1	X_2	X_3	Observed	Predicted
1[a]	*3300*	*180*	*105*	24.45	22.40
2	3300	60	180	26.27	24.22
3	5500	180	30	10.23	7.88
4[a]	*3300*	*180*	*105*	20.36	22.40
5	5500	60	105	16.59	19.03
6	5500	180	180	42.05	41.66
7	1100	300	105	23.86	21.42
8	5500	300	105	31.12	31.42
9	3300	60	30	0.86	0.77
10	1100	180	30	14.01	14.40
11	3300	300	30	6.74	8.79
12	1100	60	105	19.90	19.60
13	1100	180	180	23.35	25.70
14	3300	300	180	30.33	30.42
15[a]	*3300*	*180*	*105*	22.40	22.40

[a] *Central points.*

2.7. Statistical analysis

The coefficients corresponding to the model equation were obtained using Statgraphics Centurion XV.I. (StatPoint Technologies Inc., Warrenton, VA, USA). The analysis of variance (ANOVA) in order to determine any significant difference ($P < 0.05$) was carried out using the SPSS 21.0 software package (LEAD Technologies, Inc., Chicago, USA).

3. Results and discussion

3.1. UV-A LED photo-Fenton optimization by Response Surface Methodology

The present study was conducted to evaluate the optimal conditions for the removal of COD present in a crystallized fruit effluent (Table 1, sample C) through photo-Fenton treatment assisted with UV-A LED radiation (23 W/m^2). Nowadays, the high number of variables that affect photo-Fenton treatments, such as pH, temperature, radiation source, reaction time or dosages of H_2O_2, and Fe^{3+}/Fe^{2+} are well-known (Pignatello et al., 2006). Similarly, it is widely accepted that the optimal pH for Fenton and photo-Fenton reactions ranges from 2.5 to 3.5, since all iron added to water is dissolved at this value, increasing the formation of hydroxyl radicals (Pignatello et al., 2006). Thus, all treatments in this study were carried out at pH 3 to obtain the higher yield in terms of COD removal.

The assessment of the percentage of COD removal was made throughout a range of UV-A LED photo-Fenton conditions (n = 15) based on distinct combinations of H_2O_2 concentration, Fe^{3+} concentration, and reaction time. The results of the 15 runs are shown in Table 2b. This table includes the experimental design, as well as the observed and predicted values for the considered variable, and the percentage of COD removal. Two preliminary rounds of analytical assessment were performed in order to obtain the adequate range for the considered factors: H_2O_2 concentration (X_1: 1100–5500 mg/L), Fe^{3+} concentration (X_2: 60–300 mg/L) and reaction time (X_3: 30–180 min). The mismatch regarding the optimal values of the ranges considered in the two first rounds could have been due to a conditioning effect exerted by each factor on others and this situation prompted us to enlarge the ranges to obtain optimal values. The range of H_2O_2 and Fe^{3+} concentrations were consistent with those previously assayed in the treatment of agro-industrial effluents by other authors (Dogruel et al., 2009; Durán et al., 2011). With respect to H_2O_2 concentration, the reaction rate increases in parallel to the augment of hydrogen peroxide dosage because of the concentration of hydroxyl radicals. However, an excessive dosage of H_2O_2 may cause an adverse effect (Wang and Lemley, 2001; Maezono et al., 2011). Thus, the optimal dosage of H_2O_2 depends on the physico-chemical characteristics of the effluent and the dosage of iron (Cassano et al., 2011). Additionally, Fenton and photo-Fenton reaction rate increases with high iron concentrations due to the higher generation of hydroxyl radicals (Malato et al., 2009), although with a certain concentration of iron, the efficiency of the reaction decreases or scavenger effects can occur. For this reason a Fe/H_2O_2 ratio as small as possible is desirable in an attempt to avoid possible recombination between both and, thereby reduce the production of iron complexes. Consequently, the interconnection between factors involved in the Fenton and photo-Fenton reaction encourages the evaluation of optimal concentrations of H_2O_2 and iron to maximize the COD removal.

The quadratic model achieved permitted the adjustment of theoretical values of COD removal to observed values with a low deviation (Table 2b), suggesting a successful application of the

Response Surface Methodology as an optimization procedure. In the present study, the model employed was observed to be useful enough to predict COD removal yields without any further experiment.

The regression coefficients of intercept, linear, quadratic, and interaction terms of the model were calculated using the least square method. The effect of the linear, quadratic or interaction coefficients on the response was studied via an analysis of variance (ANOVA) (Table 3). The degree of significance of each factor is represented by its P value, which indicates that the regression models for COD removal was statistically relevant - with a level of significance ranging from $P < 0.0001$ to $P < 0.0165$. The models did not display significant lack of fit ($P > 0.05$). Thus, these statistical parameters indicated well-fitting models for the described variables. These statistical analyses revealed that the most important variable for COD was the reaction time (X_3) ($P < 0.001$), whilst secondary variation can be attributed to the Fe^{3+} concentration (X_2) and the combination of H_2O_2 and reaction time (X_1X_2) (both $P < 0.05$) (Table 3).

The response surface plots obtained further supported the relative contribution to the optimal condition for COD removal of each variable evaluated (Fig. 1), and were confirmed by the value of the coefficient of each factor obtained in the polynomial equation (Equation (3)). Moreover, the regression coefficient (R^2) for this method was 0.973, which means that the model matches the COD removal adequately.

$$Y = 8.91847 - 0.00895875X_1 + 0.0755896X_2 + 0.174102X_3 + 7.04976\cdot10^{-7}X_1^2 + 0.0000100095X_1X_2 + 0.0000340606X_1X_3 - 0.000204716X_2^2 - 0.0000505556X_2X_3 - 0.000605407X_3^2 \quad (3)$$

Optimal conditions concerning the three variables studied were achieved for the treatment of effluent C (Table 1). Thus, the optimal dosages of H_2O_2 and Fe^{3+} were 5459 and 286 mg/L, respectively. However, to obtain higher COD removal, an optimal reaction time higher than 180 min could be expected.

3.2. UV-A LED photo-Fenton

As mentioned in Table 1, due to the low BOD_5/COD ratio and the reducer behaviour of these effluents, a combination of photo-Fenton and CFD was chosen as the best alternative to increase the biodegradability of the effluent, suspended solids and turbidity removal. Different UV-A LED photo-Fenton treatments were carried out using the optimal conditions obtained through the RSM (H_2O_2 = 5459 mg/L; Fe^{3+} = 286 mg/L; time > 180 min). These optimal conditions were applied to the two UV-A LED photo-systems at pH 3 during 360 min Fig. 2a shows the COD removal after the Fenton and photo-Fenton treatment was carried out in the first UV-A LED photo-system with an irradiance of 23 W/m^2. As can be observed in Fig. 2a, photo-Fenton treatment reached a COD removal rate of around 45% after 360 min. The level of COD removal reached contrasts with the results obtained by Fenton reagent, which only afforded a degradation of 13% at the end of the treatment. In addition, as can be seen in Fig. 2a, UV-A LED irradiation assays were also carried out. From the data, it can be observed that no changes occurred after 360 min of irradiation.

In order to increase the amount of COD removal from the crystallized-fruit industry effluents, a more powerful UV-A LED photo-system was applied. This second UV-LED photo-system was characterized by a higher irradiance under the same current intensity, with the same electric consumption. Therefore, with a current intensity of around 240 mA, an irradiance of 70 W/m^2 was achieved. Additionally, in order to use the maximum capacity of the second UV-LED photo-system, a current intensity of 85 W/m^2 was applied to the effluent. Fig. 2b shows the COD removal in the crystallized fruit effluent after the application of the photo-Fenton treatment with the second UV-A LED system using the optimal conditions reached in the RSM. As shown in Fig. 2b, a higher COD removal (74%) was achieved with 85 W/m^2. This value is slightly

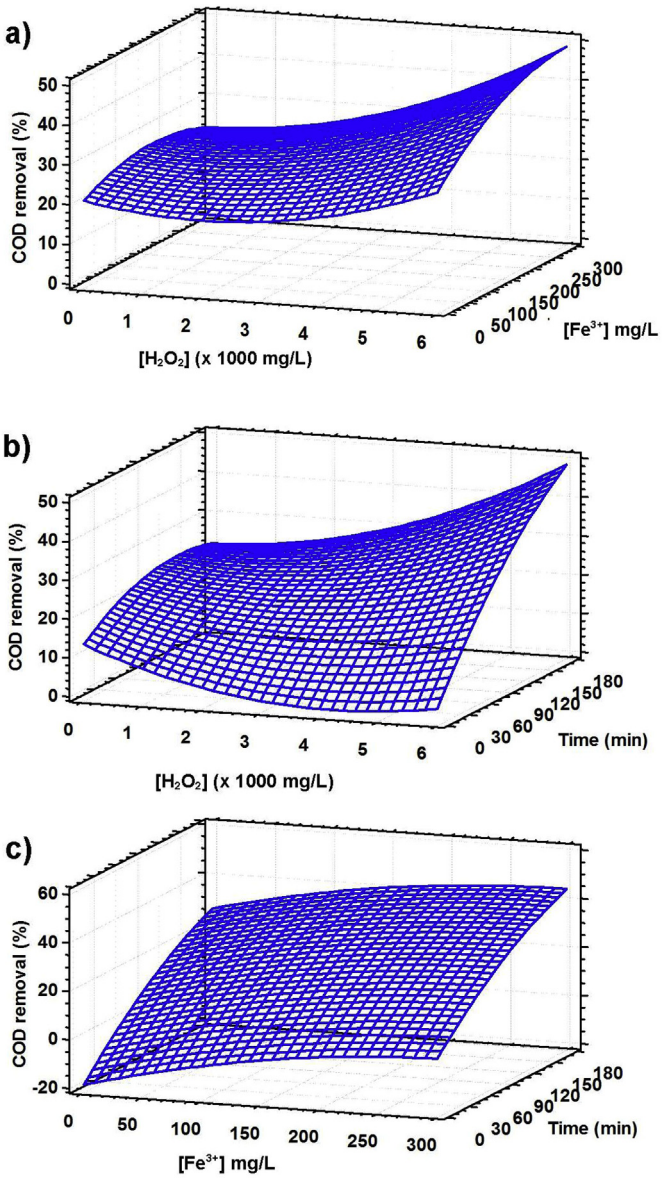

Fig. 1. Response-surface plot showing the effect of H_2O_2, Fe^{3+}, and reaction time on COD removal from crystallized-fruit effluents.

Table 3
Corresponding F-values and P-values for selected responses for each obtained coefficient.

Variable	X_1	X_2	X_3	X_1X_1	X_1X_2	X_1X_3	X_2X_2	X_2X_3	X_3X_3
F-value	5.53	12.56	126.29	5.34	3.47	15.7	3.99	0.1	5.32
P-value	n.s.	*	***	n.s.	n.s.	*	n.s.	n.s.	n.s.

X1: H_2O_2 (mg/L); X2: Fe^{3+} (mg/L); X3: Reaction time (min). n.s.: Non-significant. Significant at $^*P < 0.05$ and $^{***}P < 0.001$.

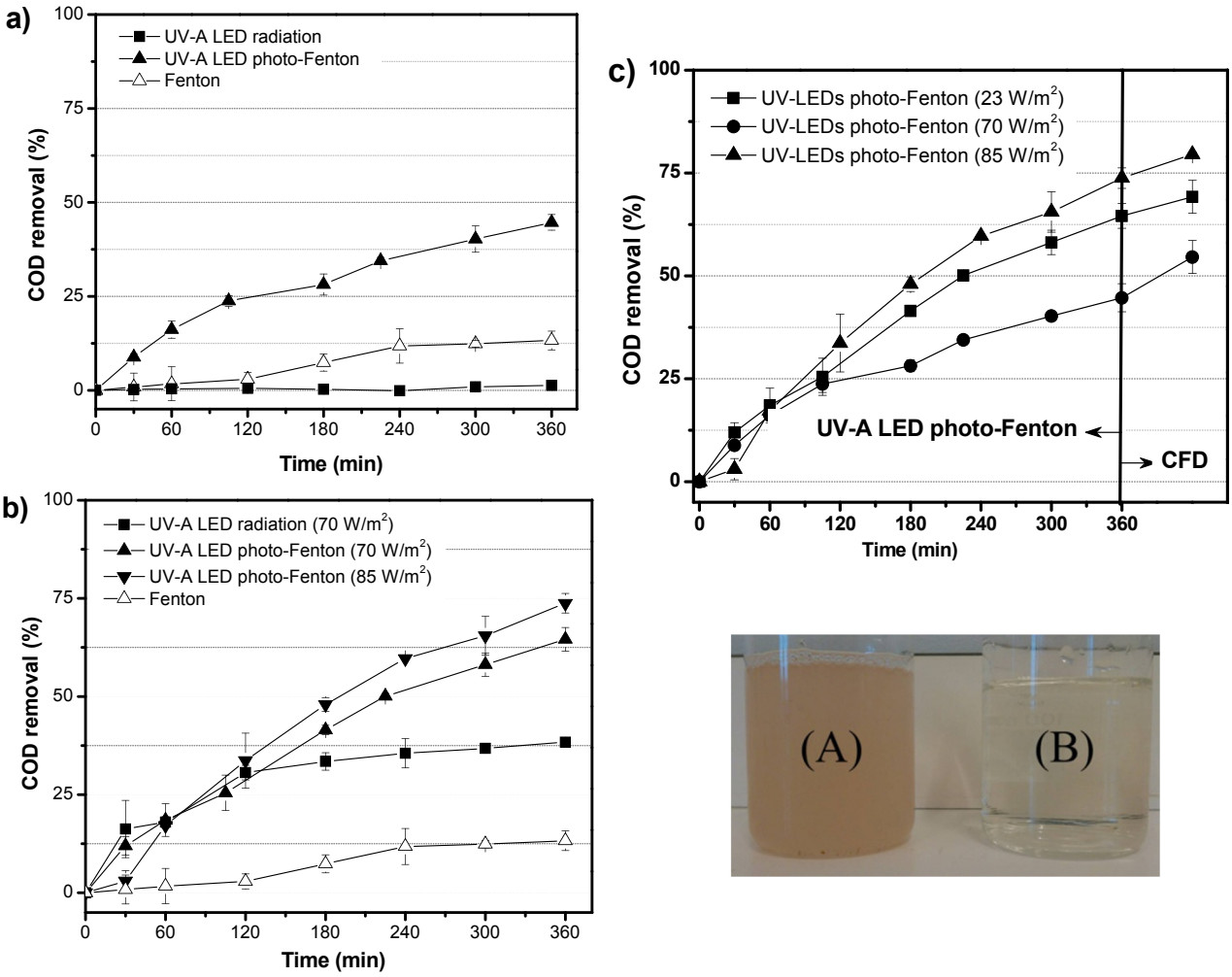

Fig. 2. COD removal with: (a) first UV-A LED photo-system; (b) with the second UV-A LED photo-system, using the optimal conditions reached in the RSM ($[H_2O_2]$ = 5459 mg/L; $[Fe^{3+}]$ = 286 mg/L; reaction time >180 min); (c) combined UV-A LED photo-Fenton/CFD processes.

higher than that obtained with an irradiance of 70 W/m^2, which was only 65%. Both values are much higher than that obtained in the Fenton treatment, in the absence of a UV-A LED irradiance (13%). On the other hand, control assays with UV-A LED irradiation and H_2O_2/UV-A LED irradiation were carried out in order to check the effect of the different variables independently. In both cases, a final COD reduction of 38% was reached after 360 min. These results mean that the combination of hydrogen peroxide with UV-A irradiation does not have an oxidation effect over the effluent, since the degradation curve is similar to that obtained in the experiment performed in the absence of H_2O_2. Therefore, all the increased reduction of organic matter is a consequence of UV-A LED irradiation. On the other hand, it is necessary to take into account the amount of consumed hydrogen peroxide in photo-Fenton treatments in comparison to the blank assays. In both photo-Fenton treatments (70 and 85 W/m^2), hydrogen peroxide was totally consumed at 120 min, and for this reason this oxidant reagent was added again at the initial concentration in order to maintain a constant concentration until the end of the reaction. Thus, approximately 22 g/L of H_2O_2 was consumed in the treatment carried out with 70 W/m^2. Whilst, approximately up to 29 g/L of hydrogen peroxide, was consumed in the treatment with a higher irradiance. As can be observed in Fig. 2b, there are small differences in the first 120 min of degradation curves for both photo-Fenton assays and UV-A LED irradiation and H_2O_2/UV-A LED irradiation, indicating that this sampling point is coincident with the consumption of the initially added hydrogen peroxide (5.4 g/L of H_2O_2). This means that the first minutes of reaction, due to the high organic load in the effluent, the main effects on the degradation of organic matter are related to the effect of irradiation and to a lesser extent associated with the hydroxyl radicals generated in photo-Fenton treatment. As the reaction proceeds, the organic load decreases and a higher amount of hydroxyl radicals are formed, causing the consumption of hydrogen peroxide and the advance in the organic matter degradation.

Durán et al. (2011) reported values of COD removal of 59% after 120 min in juice effluents with 5800 mg/L of H_2O_2 and 40 mg/L Fe^{3+}. This result is considerably higher than that shown in Fig. 2. However, it is necessary to take into account important differences between the two studies. Firstly, the effluent studied by Durán et al. (2011), had an initial COD value of 1260 mg O_2/L, much lower than that studied in this research (30 000–35 000 mgO_2/L). Secondly, photo-Fenton treatments carried out by Durán et al. (2011) were assisted with UV-C radiation (low pressure mercury lamp) emitting at λ = 190–280 nm. In contrast, UV-A radiation from LEDs lamps was used to assist photo-Fenton treatments in the present research. Velegraki and Mantzavinos (2015) reported a COD removal of around 80% of winery effluents, after 210 min, through solar photo-Fenton carried out in CPC reactors. To obtain this value an H_2O_2:COD ratio of 1.7 was used. This ratio is almost three times higher than the ratio,

(0.6), used to treat the crystallized-fruit effluents which were the object of this study. Thus, despite the complexity of the water matrix treated in the present study (higher COD concentration and reducer behaviour with negative values of redox potential), a similar COD removal to that obtained by Velegraki and Mantzavinos (2015) was achieved, together with a higher effectiveness of H_2O_2, which enabled the treatment of higher amounts of COD with the same or lower doses of hydrogen peroxide.

After the UV-A LED photo-Fenton treatments, a coupled CFD stage was carried out in order to increase the COD removal and to reduce the amount of total suspended solids and the turbidity in the treated sample. With this objective, different inorganic and organic coagulants were tested (data not shown). After studying the results obtained with the different coagulants, a coagulation–flocculation–decantation stage at pH 7 using the remaining iron ($[Fe_{total}] \approx 325$ mg/L) from photo-Fenton treatment was carried out. These conditions were selected not only with regards to COD and total suspended solids and turbidity removal, but also taking into account economic factors in order to transfer the studied treatment at laboratory scale to a real treatment plant inside the crystallized-fruit factory. Fig. 2c shows the COD removal after the coupled treatment (UV-A LED photo-Fenton and CFD) with different UV irradiances (23, 70 and 85 W/m^2). As can be seen in this figure, COD removal of treated effluents increased around 22%, with a final value 54% in the combined treatment carried out with 23 W/m^2. On the other hand, a slighter increase of around 7% was observed in those treatments carried out in the second photosystem with 70 and 85 W/m^2 achieving a 69 and 80% final removal of COD respectively. In addition, not only was organic matter removed, but high removal of turbidity and suspended solids was also achieved after the coagulation–flocculation stage. Therefore, maximum values of 99 and 95% were attained for turbidity and total suspended solids removal after both combined treatments were carried out in the second UV-A LED photo-system.

3.3. Biodegradability enhancement during coupled UV-A LED photo-Fenton and CFD treatments

A good biodegradability index of treated wastewater is required for the application of a biological process as the last step in a crystallized-fruit wastewater treatment system. The biodegradability index of all the treated samples (after UV-A LED photo-Fenton and photo-Fenton combined with CFD treatments) as well as raw wastewater, were evaluated according to the BOD_5/COD ratio. As shown in Fig. 3, effluent biodegradability increases according to the requirement of treatment. As can be observed in Fig. 3 and Table 1, the biodegradability index of the raw wastewater ranges below 0.4, between 0.06 and 0.19. Thus it could be considered as non-biodegradable effluent, since 0.4 is the value at which an effluent can be considered as being easily biodegradable (Pulgarin et al., 1999; Metcalf and Eddy, 2002; Esplugas et al., 2004).

The application of photo-Fenton treatment assisted with 23 W/m^2 of UV-A LED radiation slightly increases the biodegradability to 0.27. This value is still not enough to carry out a conventional biological treatment. However, an increase of the irradiance in the UV-A LED photo-Fenton treatments leads to the enhancement of the organic matter removal and thus an increase in the biodegradability of the treated effluent. Therefore, after the photo-Fenton treatments with 70 and 85 W/m^2 the biodegradability index of the treated effluent rises to 0.36 and 0.39, respectively. Although the effluent is near to biodegradability, it can only be considered biodegradable when the ratio exceeds 0.4. This value is exceeded after the coupling of the UV-A LED photo-Fenton system and a coagulation–flocculation step. For instance, with an irradiance of 70 W/m^2 the treated effluent had a biodegradability ratio of 0.43, while, with irradiance of 85 W/m^2 the value is 0.56 after the combined treatment. Therefore, effluents, after UV-A LED photo-Fenton and subsequent CFD treatment, can be directed to a biological treatment stage in order to achieve the total degradation of organic matter. Similar coupling treatments have been reported in our research group and by other authors (Lucas et al., 2007; Silva et al., 2013; Manenti et al., 2014).

To sum up, an effective crystallized-fruit wastewater treatment cycle could begin in a homogenization tank, where, after a pH adjustment, the UV-A LED photo-Fenton treatment takes place for enough time to degrade the organic matter to approximately 75%. Then, after being led to a secondary tank, the CFD step could be carried out at pH 7, using the remaining iron from photo-Fenton step. During this stage, turbidity and suspended solids would be removed almost completely. To finalise the process, the pre-treated

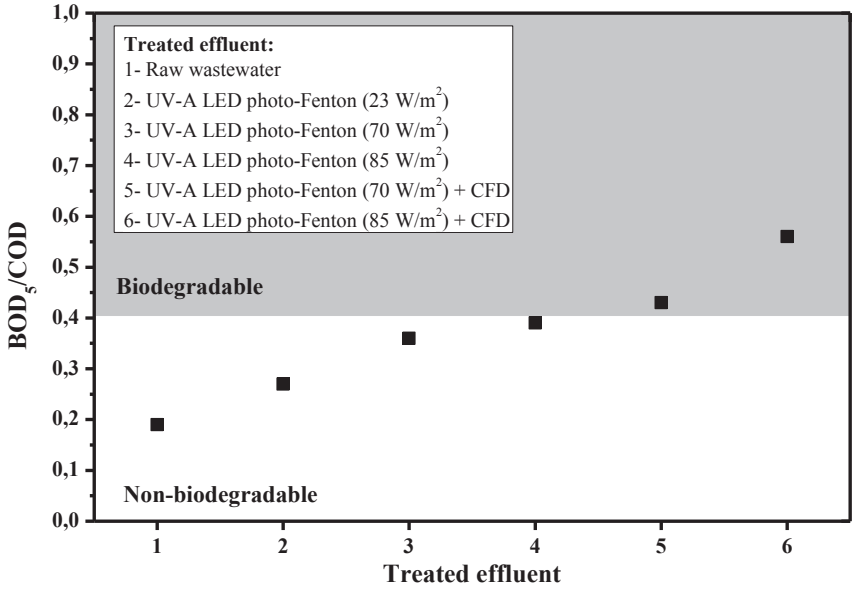

Fig. 3. Evolution of biodegradability index of treated effluents.

effluent (5000–7000 mg O_2/L) could be subjected to a biological treatment, such as an activated sludge process. The retention time in the activated sludge tank would be dependent upon the treatment goals. If the effluent is to be discharged into a MWWTP, the maximum admissible value of COD is 1000 mg O_2/L, so a lower retention time would suffice. Alternatively, if the effluent is to be discharged into a natural water course, a higher retention time in the biological treatment stage would be necessary, since the maximum admissible value is 150 mg O_2/L (Decreto-Lei no 236/98).

4. Conclusions

A Box-Behnken design of Response Surface Methodology was employed to obtain maximum organic matter removal from crystallized-fruit wastewater using a UV-A LED photo-Fenton treatment. The experimental design was effective in estimating the influence of three independent variables critically involved in the removal of COD: [Fe^{3+}], [H_2O_2], and reaction time. In addition, a quadratic model was used to predict response. Evaluation of the best combination of variables to achieve the maximum COD removal (Fe^{3+} = 286 mg/L; H_2O_2 = 5459 mg/L and reaction time >180 min) was performed using two UV-A LED photo-systems. The two UV-A LED systems allowed the evaluation of the influence of increasing the irradiance from 23 to 85 W/m^2.

UV-A LED radiation is a serious alternative to conventional UV lamps in terms of ecofriendliness, operational cost, and energy efficiency.

The COD removal increased with the irradiance intensification in the photo-Fenton treatment and 45% of organic matter was removed with a photo-Fenton with 23 W/m^2. When the second UV-A LED system was used (with 70 and 85 W/m^2) the removal of COD reached 65 and 74%, respectively.

The coupling of UV-A LED photo-Fenton and CFD increased the removal of COD, to 80% and, a higher removal of suspended solids (95%) and turbidity (99%) was also achieved.

This combined treatment process significantly improved the biodegradability index of the treated effluents, in comparison to that of the raw effluent. Consequently, after UV-A LED photo-Fenton/CFD treatment, the subsequent effluents can be subjected to conventional biological treatments, such as activated sludge, in order to achieve complete degradation of the effluent's organic matter.

Acknowledgements

The authors are grateful to the Fundação para a Ciência e a Tecnologia (FCT) for the financial support provided to CQVR through PEst-C/QUI/UI0616/2014 and to the Project INNOFOOD – NORTE-07-0124-FEDER-0000029. Marco S. Lucas acknowledges also the funding provided by the European Union's Horizon 2020 research and innovation programme under the Marie Sklodowska-Curie grant agreement No 660969.

Appendix A. Supplementary material

Supplementary material related to this article can be found at http://dx.doi.org/10.1016/j.chemosphere.2015.11.092.

References

Amor, C., De Torres-Socías, E., Peres, J.A., Maldonado, M.I., Oller, I., Malato, S., Lucas, M.S., 2015. Mature landfill leachate treatment by coagulation/flocculation combined with Fenton and solar photo-Fenton processes. J. Hazard. Mater. 286, 261–268.

Cassano, D., Zapata, A., Brunetti, G., Del Moro, G., Di Iaconi, C., Oller, I., Malato, S., Mascolo, G., 2011. Comparison of several combined/integrated biological-AOPs setups for the treatment of municipal landfill leachate: minimization of operating costs and effluent toxicity. Chem. Eng. J. 172 (1), 250–257.

Chatzisymeon, E., Foteinis, S., Mantzavinos, D., Tsoutsos, T., 2013. Life cycle assessment of advanced oxidation processes for olive mill wastewater treatment. J. Clean. Prod. 54, 229–234.

Chen, R., Pignatello, J., 1997. Role of quinone intermediates as electron shuttles in Fenton and photoassisted Fenton oxidations of aromatic compounds. Environ. Sci. Technol. 31, 2399–2406.

De Torres-Socías, E., Fernández-Calderero, I., Oller, I., Trinidad-Lozano, M.J., Yuste, F.J., Malato, S., 2013. Cork boiling wastewater treatment at pilot plant scale: comparison of solar photo-Fenton and ozone (O_3, O_3/H_2O_2). Toxicity and biodegradability assessment. Chem. Eng. J. 234, 232–239.

Decreto-Lei nº. 236/98, de 1 de Agosto. Diário da República – I Série-A. nº. 176-1-8-1998.

Dogruel, S., Olmez-Hanci, T., Kartal, Z., Arslan-Alaton, I., Orhon, D., 2009. Effect of Fenton's oxidation on the particle size distribution of organic carbon in olive mill wastewater. Water Res. 43 (16), 3974–3983.

Durán, A., Monteagudo, J.M., Carnicer, A., 2011. Photo-Fenton mineralization of synthetic apple-juice wastewater. Chem. Eng. J. 168 (1), 102–107.

Durán, A., Monteagudo, J.M., Carnicer, A., San Martín, I., Serna, P., 2012. Solar photodegradation of synthetic apple juice wastewater: process optimization and operational cost study. Sol. Energy Mater. Sol. Cells 107, 307–315.

Eaton, A.D., Clesceri, L.S., Rice, E.W., Greenberg, A.E., Franson, M.A.H., 2005. Standard Methods for the Examination of Water and Wastewater, twenty-first ed. APA-AWWA-WEF.

Esplugas, S., Contreras, S., Ollis, D.F., 2004. Engineering aspects of the integration of chemical and biological oxidation: simple mechanistic models for the oxidation treatment. J. Environ. Eng. 130 (9), 967–974.

Kuo, W.G., 1992. Decolorizing dye wastewater with Fenton's reagent. Water Res. 26 (7), 881–886.

Lanao, M., Ormad, M.P., Goñi, P., Miguel, N., Mosteo, R., Ovelleiro, J.L., 2010. Inactivation of *Clostridium perfringens* spores and vegetative cells by photolysis and TiO_2 photocatalysis with H_2O_2. Sol. Energy 84 (4), 703–709.

Lanao, M., Ormad, M.P., Mosteo, R., Ovelleiro, J.L., 2012. Inactivation of *Enterococcus sp.* by photolysis and TiO_2 photocatalysis with H_2O_2 in natural water. Sol. Energy 86, 619–625.

Lucas, M.S., Dias, A.A., Sampaio, A., Amaral, C., Peres, J.A., 2007. Degradation of a textile reactive Azo dye by a combined chemical–biological process: Fenton's reagent-yeast. Water Res. 41 (5), 1103–1109.

Lucas, M.S., Peres, J.A., Amor, C., Prieto-Rodríguez, L., Maldonado, M.I., Malato, S., 2012. Tertiary treatment of pulp mill wastewater by solar photo-Fenton. J. Hazard. Mater. 225–226, 173–181.

Maezono, T., Tokumura, M., Sekine, M., Kawase, Y., 2011. Hydroxyl radical concentration profile in photo-Fenton oxidation process: generation and consumption of hydroxyl radicals during the discoloration of azo-dye Orange II. Chemosphere 82, 1422–1430.

Malato, S., Fernández-Ibáñez, P., Maldonado, M.I., Blanco, J., Gernjak, 2009. Decontamination and disinfection of water by solar photocatalysis: recent overview and trends. Catal. Today 147, 1–59.

Manenti, D.R., Módenes, A.N., Soares, P.A., Espinoza-Quiñones, F.R., Boaventura, R.A.R., Bergamasco, R., Vilar, V.J.P., 2014. Assessment of a multistage system based on electrocoagulation, solar photo-Fenton and biological oxidation processes for real textile wastewater treatment. Chem. Eng. J. 252, 120–130.

Metcalf, Eddy, 2002. Wastewater Engineering: Water and Reuse. McGraw-Hill, Inc., New York.

Mosteo, R., Miguel, N., Martín-Muniesa, S., Ormad, M.P., Ovelleiro, J.L., 2009. Evaluation of trihalomethane formation potential in function of oxidation processes used during the drinking water production process. J. Hazard. Mater. 172 (2–3), 661–666.

Natarajan, K., Natarajan, T.S., Bajaj, H.C., Tayade, R.J., 2011. Photocatalytic reactor based on UV-LED/TiO_2 coated quartz tube for degradation of dyes. Chem. Eng. J. 178, 40–49.

Peres, J.A.S., Carvalho, L.H.M., Boaventura, R.A.R., Costa, C.A.V., 2004. Characteristics of p-hydroxybenzoic acid oxidation using Fenton's reagent. J. Environ. Sci. Health A 39, 1–17.

Pignatello, J.J., Oliveros, E., MacKay, A., 2006. Advanced oxidation processes for organic contaminant destruction based on the Fenton reaction and related chemistry. Crit. Rev. Environ. Sci. Technol. 36, 1–84.

Polo-López, M.I., Fernández-Ibáñez, P., Ubomba-Jaswa, E., Navntoft, C., García-Fernández, I., Dunlop, P.S.M., Schmid, M., Byrne, J.A., McGuigan, K.G., 2011. Elimination of water pathogens with solar radiation using an automated sequential batch CPC. J. Hazard. Mater. 196, 16–21.

Pulgarin, C., Invernizzi, M., Parra, S., Sarria, V., Polania, R., Péringer, P., 1999. Strategy for the coupling of photochemical and biological flow reactors useful in mineralization of biorecalcitrant industrial pollutants. Catal. Today 54, 341–352.

Rodríguez-Chueca, J., Mosteo, R., Ormad, M.P., Ovelleiro, J.L., 2012. Factorial experimental design applied to *Escherichia coli* disinfection by Fenton and photo-Fenton processes. Sol. Energy 86, 3260–3267.

Rodríguez-Chueca, J., Polo-López, M.I., Mosteo, R., Ormad, M.P., Fernández-Ibáñez, P., 2014. Disinfection of real and simulated urban wastewater effluents using a mild solar photo-Fenton. Appl. Catal. B Environ. 150–151, 619–629.

Rojviroon, T., Laobuthee, A., Sirivithayapakorn, S., 2012. Photocatalytic activity of toluene under UV-LED light with TiO_2 thin film. Int. J. Photoenergy. http://

dx.doi.org/10.1155/2012/898464.
Sichel, C., Blanco, J., Malato, S., Fernández-Ibáñez, P., 2007. Effects of experimental conditions on *E. coli* survival during solar photocatalytic water disinfection. J. Photochem. Photobiol. A Chem. 189, 239–246.
Silva, T.F.C.V., Silva, M.E.F., Cunha-Queda, A.C., Fonseca, A., Saraiva, I., Sousa, M.A., Gonçalves, C., Alpendurada, M.F., Boaventura, R.A.R., Vilar, V.J.P., 2013. Multi-stage treatment system for raw leachate from sanitary landfill combining biological nitrification–denitrification/solar photo-Fenton/biological processes, at a scale close to industrial – biodegradability enhancement and evolution profile of trace pollutants. Water Res. 47 (16), 6167–6186.
Singleton, V.L., Rossi, J.A., 1965. Colorimetry of total phenolics with phosphomolybdic phosphotungstic acid reagents. Am. J. Enol. Vitic. 16, 144–158.
Velegraki, T., Mantzavinos, D., 2015. Solar photo-Fenton treatment of winery effluents in a pilot photocatalytic reactor. Catal. Today 240, 153–159.
Walling, C., 1998. Intermediates in the reactions of Fenton type reagents. Acc. Chem. Res. 31 (4), 155–157.
Wang, S., Guan, Y., Wang, L., Zhao, W., He, H., Xiao, J., Yang, S., Sun, C., 2015. Fabrication of a novel bifunctional material of BiOI/Ag_3VO_4 with high adsorption–photocatalysis for efficient treatment of dye wastewater. Appl. Catal. B Environ. 168–169, 448–457.
Wang, Q., Lemley, A.T., 2001. Kinetic model and optimization of 2,4-D degradation by anodic treatment. Environ. Sci. Technol. 42 (3–4), 219–224.